

## POWDER FLOW WITHIN A PHARMACEUTICAL TABLET PRESS – A DEM ANALYSIS

CLAUDIA HILDEBRANDT<sup>1,\*</sup>, SRIKANTH R. GOPIREDDY<sup>2</sup>, REGINA SCHERLISS<sup>1</sup> AND NORA A. URBANETZ<sup>2</sup>

<sup>1</sup> Department of Pharmaceutics and Biopharmaceutics  
Christian-Albrechts-University Kiel, Grasweg 9a, 24118 Kiel, Germany  
e-mail: childebrandt@pharmazie.uni-kiel.de, rscherliess@pharmazie.uni-kiel.de  
web page: <http://www.uni-kiel.de/Pharmazie/technologie/>

<sup>2</sup> Daiichi-Sankyo Europe GmbH  
Pharmaceutical Development, Luitpoldstr. 1, 85276 Pfaffenhofen, Germany  
e-mail: Srikanth.Gopireddy@daiichi-sankyo.eu, Nora.Urbanetz@daiichi-sankyo.eu  
web page: <https://www.daiichi-sankyo.eu/>

**Key words:** DEM analysis, pharmaceutical tableting, die filling, force feeder

**Abstract.** Numerical simulations in pharmaceutical industry are gaining importance as an advanced tool to elucidate the underlying physics in unit operations during tablet manufacturing. Out of different processing stages, powder flow within the tableting machine constitutes one critical step defining inter alia product safety in terms of content and content uniformity of the active pharmaceutical ingredient (API). By means of numerical simulations the Quality by Design (QbD) approach could be integrated to enhance product quality. However, the numerical simulations reported so far either evaluated the powder flow in a simplified system without considering the complex geometrical configuration within the rotary tablet press or used unrealistic micro-mechanical particle properties and sizes.

This work presents a numerical approach for studying the powder flow within a force feeder to die/cavity in a rotary tablet press with actual dimensions to evaluate the final product quality. The computations were carried out using an open source discrete element method (DEM) code. The investigated system consists of a hopper, a force feeder comprising three rotating paddle wheels, and a turret with 24 dies. A poly-disperse particle size distribution was used mimicking a low dose direct compression formulation with calibrated micro-mechanical material properties. First of all, a summary of the basic metrics such particle size distribution and mass hold up in the different parts of the feeder is provided. Subsequently emphasis is given to the powder flow patterns in the force feeder that are visualized by particles' coloring. Results reveal that (1) the powder feeding from the hopper into the feeder shows a gradient across the feeding hopper width causing an intriguing particle mixing, (2) particles are unequally refed from dosing wheel zone and (3) an intermixing between the reverse dosing and filling wheel zone can be identified. Those three visualized powder flow phenomena are supported by quantitative analysis and eventually their influence on the filled dies is being explained.

In conclusion, this study helps in visualizing powder flow in a pharmaceutical tablet press disclosing astonishing particle flow phenomena that have not been reported yet.

## 1 INTRODUCTION

Solid dosage formulations, in particular tablets, constitute the most important application route to deliver active pharmaceutical ingredients (API) to patients. Different quality attributes have to be met to ensure patient safety. Those requirements for tables are friability, resistance to crushing, disintegration, dissolution, and uniformity of dosage units [1]. “Quality is built into products by design” [2], cited from the ICH guideline Q8 and Quality by Design (QbD) paradigm, in other words, quality can be improved by implementation of science-based manufacturing of pharmaceuticals. During tablet production on rotary tablet presses, three different steps are intertwined with each other and with the quality requirements. Those steps are the filling of powder through feeders into the dies, powder compaction, and finally tablet ejection. The first process step is achieved through material transfer by force feeders differing in terms of geometry, e.g. number and shape of paddle wheels.

QbD can be realized e.g. by numerical means of the discrete element method (DEM). This technique, in contrast to experiments, benefits of a high resolution on a particle level. However this already implies the inherent drawback of a high computational cost. Hence, most numerical studies reporting the die filling process focus on the effect of geometry design, process parameters, and micro-mechanical material properties [3, 4, 5]. Recent studies explain die filling into rotating dies by gravity [3,4] and force feeding containing different number of paddle wheels [5, 6]. Though the essential role of differently sized particles in pharmaceutical blends is only reported by few studies [4, 6].

In this work the die filling process in the context of a lab-scale rotary tablet press consisting of a filling system with three paddle wheels is investigated by DEM. Moreover a poly-disperse particle size distribution (PSD) is considered mimicking a direct compressible (DC) blend. The PSD reflects a mixture of excipients and API particles that is being compressed without prior granulation thereby emphasizing the importance of powder flowability as a whole [7]. The excipients in DC formulations are responsible for tablet dissolution in the gastrointestinal tract, flow aid, and bulk mass increase. With this given realistic system, light is shed on the die filling process and different means of process understanding are provided.

## 2 METHODOLOGY

The methodology used has already been reported in [8]. In brief, the methodology is as follows.

### 2.1 Discrete element method

After introduction of the DEM in 1979 it has evolved to a well-known approach in particle technology. This numerical model captures the trajectories of each and every particle in the system through Newton’s equation of motion. Details about theory and algorithms are described in detail in [9, 10, 11]. All computations were performed using the open source DEM software LIGGGHTS [12], version 3.4.1. Same models to calculate normal, tangential, and non-contact forces as [3, 4] have been used.

## 2.1 Geometrical setup

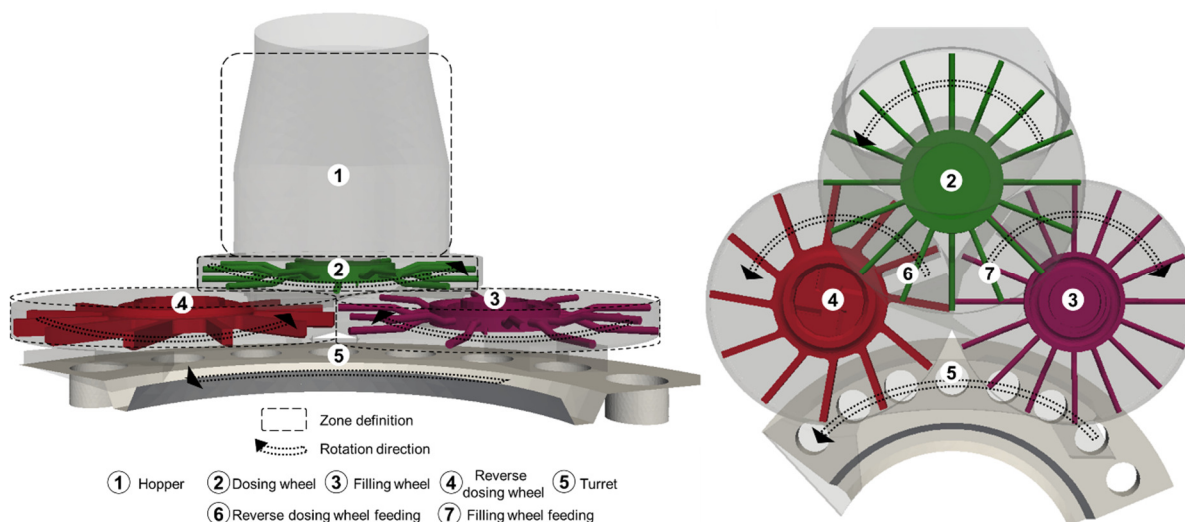


**Figure 1:** Illustration of the geometrical setup in front-(left) and top-(right) view.

The geometrical configuration and dimensions correspond to the “Fill-O-Matic” of a lab-scale FETTE 1200i rotary tablet press (Fette Compacting GmbH, Schwarzenbeck, Germany), and are illustrated in Fig. 1. It consists of a feeding hopper (① in Fig. 1) and a feeding plate consisting of three differently shaped paddle wheels. The dosing wheel (② in Fig. 1), reverse dosing wheel (④ in Fig. 1), and turret (⑤ in Fig. 1) are rotating in anti-clockwise, the filling wheel (③ in Fig. 1) in clockwise direction.

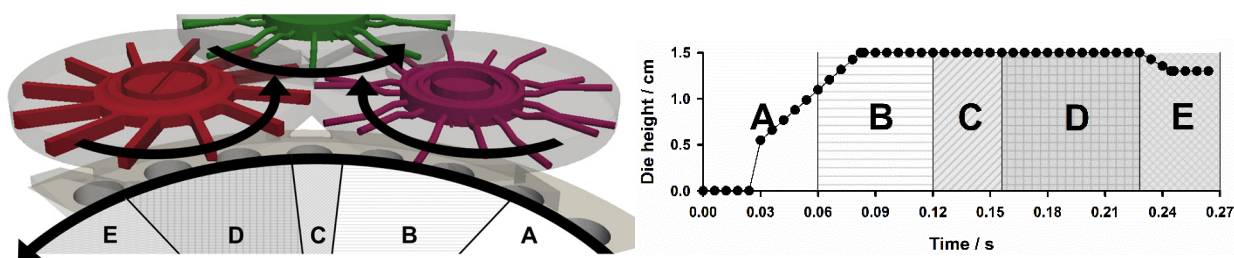


**Figure 2:** (Left) Illustration of die filling positions within Fill-O-Matic. Arrows indicate rotation direction of turret and paddle wheels. (Right) According die height at different die positions.

While the die diameter of 2.4 cm is constant, the die height is changing according to the die position during filling (Fig. 2). Initially, at the positioning of the filling wheel (“B” in Fig. 2), the lower punch is lowering during “fill cam” by 18.3 cm/s to create a maximal die height of 1.5 cm, and it remains constant (1.5 cm) during “C” and “D” in Fig. 2. At the end of filling, during “dosing cam”, the lower punch is moving upwards by 0.2 cm at 12.2 cm/s to remove excess powder and to create a more confined powder bed (“E” in Fig. 2).

## 2.2 Material properties

As mentioned in the introduction, a PSD, shown in Fig. 3, reflecting a blend consisting of API and excipient particles was defined. For excipients, six different particle sizes ranging from 1000 – 2800  $\mu\text{m}$  diameter at mean diameter of 2201  $\mu\text{m}$  were selected. In DC formulations, API particles' flowability and compressive properties limit its maximal content [7]. A reasonable content of 5% and size ratio of 1:2 to excipients' mean diameter (API particle diameter of 1129  $\mu\text{m}$ ) [13] were chosen. Although absolute particle sizes used in simulations are much higher compared to true DC blends, the total number of simulated particles ( $\sim 286,000$ ) is already at the computational limit.

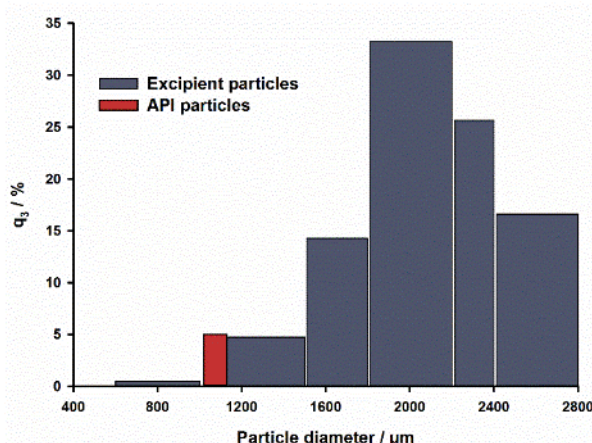


**Figure 3:** Particle size distribution consisting of 7 different sizes, out of which one particle size reflects API particles and the remaining are excipient particles of 2201  $\mu\text{m}$  mean diameter.

Bulk density, angle of repose, and mass flow rate according to Ph. Eur. [1] of different pharmaceutical diluents (different grades of lactose, mannitol, and microcrystalline cellulose used in DC formulations) have been measured. Values obtained through experiments have been compared to numerical results, and micro-mechanical properties, especially non-contact force (represented by cohesion energy density (CED)) and friction between particles and geometry (coefficient of friction, particle-wall) have been adapted iteratively to obtain good results accordance. The adapted micro-mechanical properties used during filling and discharge are within the range of literature data [3-6], and are listed in Table 1.

**Table 1:** Material properties, the numbers in parenthesis correspond to steps in Table 2.

Parameter / Unit	Property of	Value during filling (①-③)	Value during discharge (④)
Young's modulus / GPa	Particle	8.7	8.7
	Wall	210	210
Poisson's ratio / -	Particle	0.30	0.30
	Wall	0.35	0.35
Coefficient of restitution / -	Particle-particle	0.15	0.15
	Particle-wall	0.15	0.15
Coefficient of friction / -	Particle-particle	0.35	0.40
	Particle-wall	0.30	0.25
Cohesion energy density (CED) / $\text{MJ/m}^3$	Particle	1.5	1.0

## 2.3 Initialization and die filling process

The system was filled with particles according to real experiments by a step-wise procedure, listed in Table 2. At the very beginning, powder was filled from the blending container into the feeding system hopper (step no. ①, Table 2). Subsequently, powder was distributed evenly

within the Fill-O-Matic by slow paddle wheel rotations (❷, Table 2). Afterwards, the complete tableting machine was filled with powder by one turret rotation at low speed (❸, Table 2). Eventually after a physical time of 15.8 s, the completely filled system with particles is illustrated in Fig. 4.

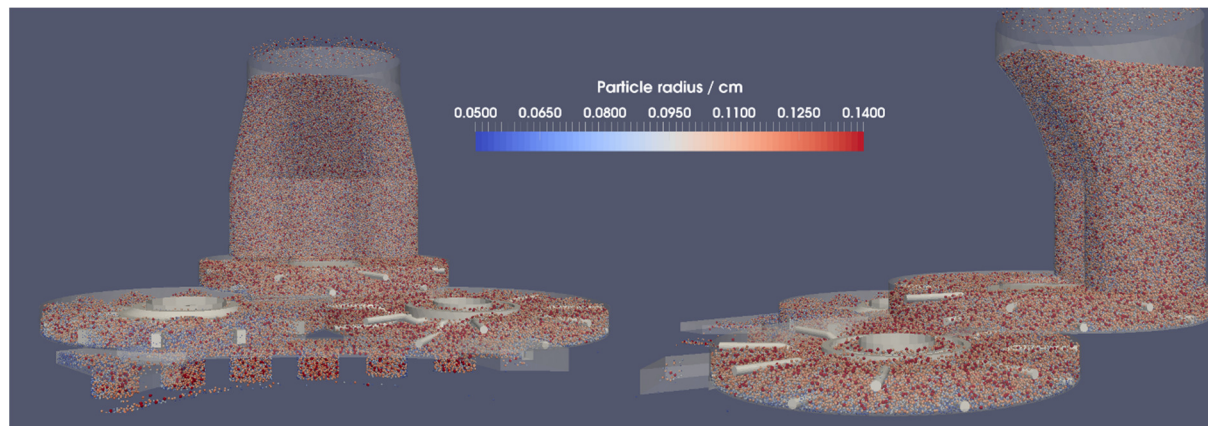


**Figure 4:** System at the end of filling (❸) and before discharge (❹) (Table 2)  
(left: front view, right: side view).

This filling procedure ensures constant filling level independent of subsequent process parameters and material properties (Table 1). Discharge or actual die filling process started by high speed tableting at increased paddle wheel speed (30 rpm) and turret speed (75 rpm) to generate a maximal output of 108,000 tablets/hour with 24 punch stations. To get an understanding of die filling during high speed tableting, ten turret revolutions to fill in total 240 dies have been performed. As particles filled in dies leave the simulation domain, continuous particles' refilling in the feeding hopper ensured constant mass in the system.

**Table 2:** Process parameters at different computation steps

No.	Description	Physical time / s	Turret speed / rpm	No. of turret rotations / -	Paddle wheel speed / rpm	No. of paddle wheel rotations / -
❶	Filling of hopper	0.8	0	0	0	0
❷	Filling of Fill-O-Matic	9	0	0	15	2.26
❸	Filling of turret	6	10	1	15	1.5
❹	Discharge	8	75	10	30	4

### 3 RESULTS AND DISCUSSION

The die filling process in an actual lab-scale pharmaceutical tablet press (FETTE 1200i) has been studied with a PSD typically found in DC formulations and with calibrated material properties. The filling of the Fill-O-Matic, following the standard procedure in experiments, and the die filling in high speed tableting at one selected combination of process parameters, namely paddle wheel and turret speed has been discussed extensively in [8]. The main focus of this manuscript will be laid on powder flow phenomena within the filling system.

### 3.1 Summary of basic die filling metrics

In [8] it has been shown, that not only during system filling but also during the die filling process, different mass hold up and particle size distributions as well as API contents, are generated at different locations of the Fill-O-Matic. The particles collected in the die originate from different positions within the Fill-O-Matic attributed to the turret rotation direction, mass flow rate from paddle wheel zones, and the die height (confer 2.1 and Fig. 2) which is only at its maximum height during rotation underneath the filling wheel zone (“B” in Fig. 2). As a result 50%, 14%, and 36% of the mass in the die stems from the filling wheel (“B”), the inter wheel (“C”), and the reverse dosing wheel (“D”) zone, respectively. In totality, a constant API content and tablet mass over production time fluctuating within the range of mean  $\pm$  one standard deviation are obtained [8].

In addition to the basic die filling metrics as described in [8], powder flow phenomena will be visualized qualitatively as well as quantitatively in the context of die filling process in the following.

### 3.2 Particle rearrangement in the system

Numerical simulations give the opportunity to look inside a given system, which is one of the major advantages compared to experiments. To visualize the powder flow within the Fill-O-Matic, the particles have been assigned different colors at the time point of discharge ( $t = 15.8$  s, ④ Table 2, Fig. 5), to see the temporal development of flow pattern within various zones of the whole system. Particles that are located in the dosing wheel zone (②, Fig. 1) are colored in green, in the filling wheel zone (③, Fig. 1) in pink, and the reverse dosing wheel zone in red (④, Fig. 1), respectively, as shown in Fig. 5. In addition to the paddle wheel zones, four additional horizontal zones in the feeding hopper (①, Fig. 1) have been created (Fig. 5A), to identify dead zones, if any exist. The rest of the particles are assigned blue color.

Three different main powder flow phenomena can be elucidated during die filling. (1) From Fig. 5A it becomes visible that the powder

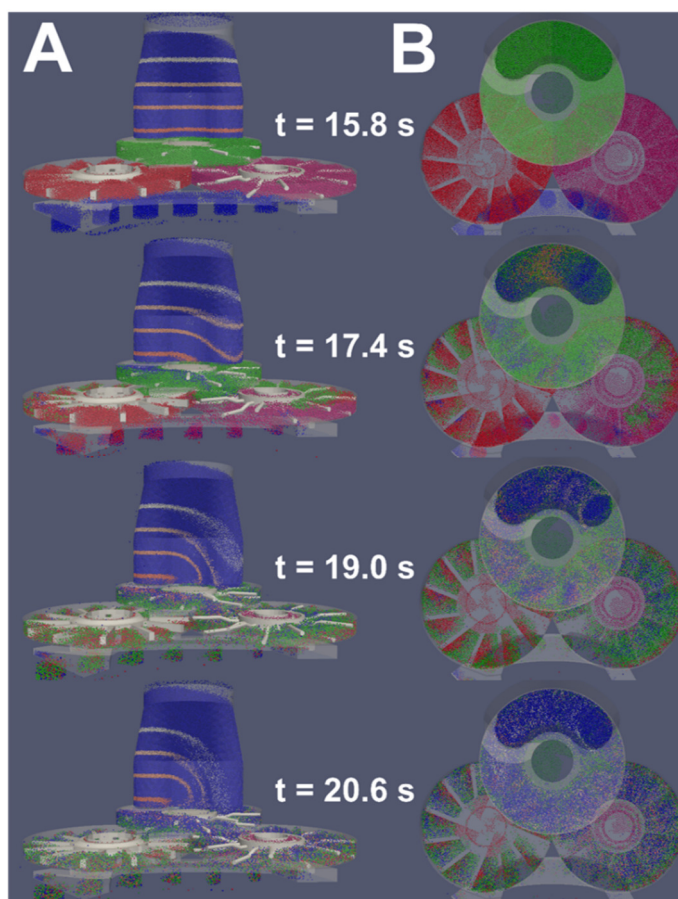


**Figure 5:** Coloring of the particles according to their initial position at time point of discharge ( $t = 15.8$  s). Particles in the paddle wheel zones are assigned different colors in addition to four horizontal zones in the feeding hopper. Colored particles are tracked over time for the for the first 6 turret rotations at every 2<sup>nd</sup> rotation ( $t = 17.4$  s for 2<sup>nd</sup>,  $t = 19.0$  s for 4<sup>th</sup>,  $t = 20.6$  s for 6<sup>th</sup> rotation, respectively). (A) Front-view, (B) top-view.

feeding from the hopper into the Fill-O-Matic shows a gradient across the feeding hopper radius causing an intriguing particle mixing. Thereby particles that are located in the left half of the hopper tend to remain there (indicating a dead zone) throughout the complete discharge period since solely the particles from right hand side enter and refill the dosing wheel zone. The other two phenomena are visualized in Fig. 5B. (2) Less particles from the dosing wheel zone are refilling through the smaller feeding zone in ⑥ compared to ⑦ (refer Fig. 1), thereby less “green” colored particles are found in the reverse dosing wheel compared to the filling wheel zone (confer e.g. time point 17.4 s and 19.0 s in Fig. 5B). (3) Furthermore an intermixing between the two bottom paddle wheels can be identified. Underneath the dosing wheel zone, particles from the reverse dosing wheel zone (“red”) and particles from the filling wheel zone (“pink”) are interchanging from one zone into the other. This interchanging is found at the outer radial location. In the following, those three identified particle flow phenomena as illustrated in Fig. 5 are quantitatively evaluated.

### 3.3 Powder flow in the feeding hopper

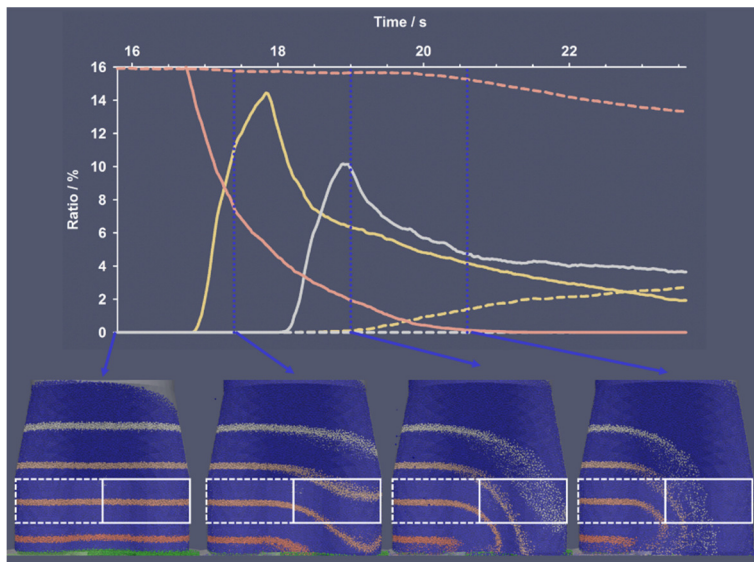


**Figure 6:** Qualitative distribution of colored particles in the middle part of the hopper, split into the left (dashed lines) and right (solid lines) half. Top: number frequency of colored particles; bottom: illustration of the system at 1.6 s intervals (15.8 s, 17.4 s, 19.0 s, and 20.6 s)

As already shown by particles coloring in Fig. 5A, particles are non-uniformly fed from the hopper into the dosing wheel zone. Four particle layers with a height of 0.5 cm were colored in grey, yellow, light orange, and dark orange, separated by zones of non-colored particles (dark blue, height of 2.5 cm). The colored particles zones as illustrated in Fig. 6 (bottom) are quantitatively analyzed over time for the middle part of the hopper (Fig 6, top) The hopper is split into a left (dashed lines), and right (solid lines) half and the number frequency of colored particles appearing in this zone are plotted over discharge time (Fig. 6, top).

At the beginning ( $t = 15.8$  s) 16% light orange colored particles are found both in left and right half of the hopper. Over time in the left half, the number frequency of light orange colored particles decreases only slightly ending with a minimum frequency of 13.8% ( $t = 23.7$  s). As soon as light orange colored particles start to deplete, yellow colors from layers above appear at  $t = 18.2$  s. In contrast to the left hopper half, completely different colored particles distribution is found in the right half. A very steep decrease of light orange colored particles with a parallel increase of yellow colored particles from layers above can be identified ( $t = 16.8$  s). Moreover, as soon as those yellow colored particles start to disappear after their maximum at  $t = 17.8$  s, the number frequency of grey colored particles increases.

At the end of discharge ( $t = 23.7$  s), the left half of the hopper still contains initially located particles (light orange) indicating a dead zone. Particles in this zone may get consolidated over time as a result of the pressure exerted by the overlying powder bed in the feeding hopper and blending container. In contrast the right half has an increased mass throughput and particles over a hopper height of  $> 10$  cm are fed into the dosing wheel zone. The reason being, as the dosing wheel is rotating in anti-clockwise direction (confer Fig. 1) underneath the hopper, main refeeding is achieved at the right half of the hopper. In follow up analysis the gradient and dead zone within the hopper have to be analyzed with respect to particle size segregation.

### 3.3 Particle refeeding

The second particle flow phenomenon as described in 3.2 and visualized in Fig. 5B, is the unevenly refeeding of particles from the dosing wheel (Fig. 1, ②) into the filling wheel (Fig. 1, ③) and reverse dosing wheel (Fig. 1, ④) zone. The number frequencies of green colored particles from the dosing wheel zone in the different paddle wheel zones over time are plotted in Fig. 7 (line colors according to paddle wheel zones, Fig. 1). Initially, all particles in the dosing wheel zone are colored in green (100% at  $t = 15.8$  s). Over time they are depleting as result of refeeding into paddle wheel zones below (③ & ④ in Fig. 1) through refeeding holes (⑦ & ⑥) at the bottom of the dosing wheel zone. In parallel differently colored particles originating from hopper emerge (data not shown).

Right at the beginning of die filling ( $t = 15.8$  s), green colored particles start to show up in filling wheel and reverse dosing wheel zone. However, a steeper increase and a higher maximal value in the filling wheel zone can be identified (max. of 54% and 42% at  $t = 18.4$  s and  $19.6$  s in filling wheel and reverse dosing wheel zone, respectively). The first explanation can be given by an increased mass flow rate that can be obtained through the larger refeeding hole into the filling wheel (⑦ in Fig. 1) compared to reverse dosing wheel zone (⑥ in Fig. 1). Second a higher mass throughput in the filling wheel zone requires a higher and faster refeeding. The increased mass throughput for the filling wheel zone is already shown in [8] by a 3-fold higher mass flow rate into the die and a 1.4-fold increased die mass contribution compared to the reverse dosing wheel zone (confer [8] and 3.1). The higher mass throughput in the filling wheel zone is also reflected by a steeper decrease of green colored particles after  $t = 18.4$  s (Fig. 7).

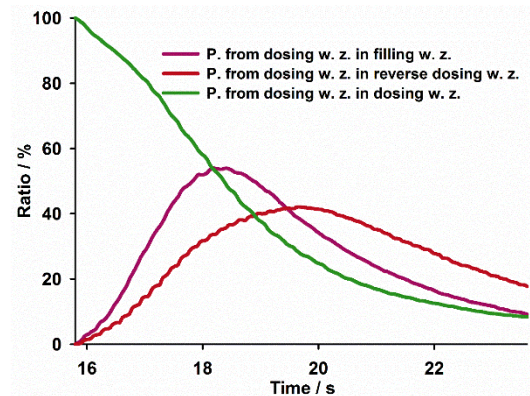


**Figure 7:** Number frequency of colored particles from dosing wheel zone (green in Fig. 5) in different locations of the Fill-O-Matic. Line colors: Green in dosing wheel, pink in filling wheel, and red in reverse dosing wheel zone.



### 3.4 Mixing between filling and reverse dosing wheel zone

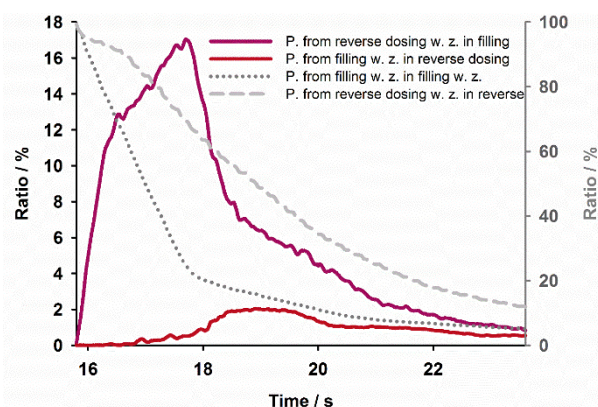


**Figure 8:** Grey lines: Number frequency of originally located particles and their depletion in filling (dotted) and reverse dosing (dashed) wheel zone. Colored lines: Number frequency of particles from reverse dosing in filling wheel zone (pink) and of particles from filling in reverse dosing wheel zone (red).

dosing wheel zone within this zone is implied (grey dashed line in Fig. 8). In summary, particles tend to remain a significantly increased residence time within the reverse dosing wheel zone. Thereby more shear forces are exerted on particles which could bear the risk for particle attrition and over lubrication [5]. Those particles from reverse dosing wheel zone enter the die at last (confer Fig. 2) hence particles in the die and over the die height have experienced different shearing history which could potentially lead to tablet capping [4].

The second approach indicating the intermixing effect (3.2) is given by the solid colored lines in Fig. 8, showing the appearance of initially located particles from the filling in the reverse dosing wheel zone (red, Fig. 8) and from the reverse dosing in the filling wheel zone (pink, Fig. 8). At the level of the two bottom paddle wheel zones and underneath the dosing wheel zone, an unclosed intersection of 4.6 cm width is found that allows free particle motion across the filling and reverse dosing wheel zones (Fig. 1). A higher particle transfer from the reverse dosing into the filling wheel zone is found with a maximum contribution of 16.7% at  $t = 17.6$  s (Fig. 8, pink). The reason being, the high mass throughput in the filling wheel zone (confer 3.3) requires a higher refeeding rate which cannot be caught up by refeeding from the dosing wheel zone. Thereby the reduced mass hold up is compensated by the mass exchange from reverse dosing wheel zone. Furthermore, the significantly reduced mass flow rate into the die from the reverse dosing wheel zone (confer [8] and 3.1) requires less refeeding hence only few particles originating from the filling wheel zone show up (2% at  $t = 18.9$  s, Fig.8, red). It also gives explanation for the two differing curve slopes of particles from filling wheel zone in the same one (grey dotted line in Fig. 8, confer above). Particles that travel from the filling into the reverse dosing wheel zone can in parallel travel back into the former one. Hence they show up again in the filling wheel zone compensating the particle depletion by discharge into the die leading to a less steep curve of the slope (grey dotted line in Fig. 8 for  $t > 17.8$  s).

Not only a different refeeding rates of the two bottom paddle wheel zones could be shown (3.3) but also an intermixing between them is indicated by particles coloring in Fig. 5B. To quantitatively evaluate this observation, two different comparisons are described in the following.

First, the grey lines in Fig. 8 reflect the depletion of originally located particles in the filling (dotted) and reverse dosing (dashed) wheel zone. Within the first 2 s of discharge ( $t = 17.8$  s) a very steep decrease of initially located particles in the filling wheel zone (pink in Fig. 5B, dotted grey line in Fig. 8) followed by a moderate decrease to a final frequency of 7.8% is found (confer below). In contrast, a sigmoidal decrease of particles from reverse

### 3.5 Colored particles in dies

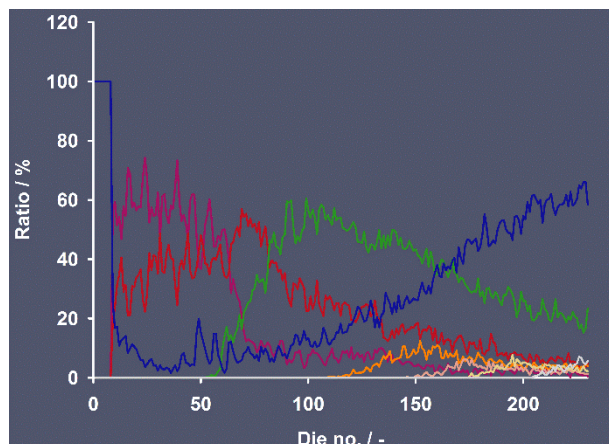


**Figure 9:** Number frequency of colored particles (confer Fig. 5 for initial position of colored particles) in the dies.

Last but not least, the appearance of colored particles in the filled dies is illustrated in Fig. 9 (confer Fig. 5 for initial position of colored particles). The first dies (1-8) have already been filled during turret filling stage (Table 2, ③) being assigned to blue color. Die no. 9-13, the first filled dies at high turret speed, (Table 2, ④) are mainly being filled by particles from filling ( $\sim 60\%$ , pink) and reverse dosing ( $\sim 30\%$ , red) wheel zone attributed to their different mass flow rates (confer 3.1). The low contribution of blue colored particles in those dies arises from particles that are initially located between Fill-O-Matic and turret (confer Fig. 5,  $t = 15.8$  s).

The first particles from the dosing wheel zone appear in die no. 53 ( $t = 17.6$  s), at the time point when almost maximum contribution of particles from dosing in filling wheel zone (confer Fig. 7, pink) is found. Red colored particles increase from the initial contribution of  $\sim 30\%$  until a maximum of  $57\%$  in die no. 61 ( $t = 18.1$  s) followed by a descent decrease until last filled die. Although the contribution of filled mass by reverse dosing wheel is only  $36\%$  (confer 3.1 and [8]) the observed maximum can be explained by the high particle exchange from the reverse dosing into filling wheel zone (confer 3.4 and Fig. 8). A constant increase of blue colored particles from the feeding hopper is found from die no. 50 ( $t = 17.7$ ). Subsequently the horizontal colored zones from the feeding hopper (confer Fig. 5A and 6) with orange, light orange, yellow, and grey particles appear in die no. 108, 142, 168, and 197, respectively.

In summary, particles that are filled into the dies have travelled a different distance within the system and originate from different locations within the Fill-O-Matic. Thereby the first filled dies contain particles that have been exerted to less shear forces [5] which could result in different compressive properties thus tablet hardness and dissolution profiles. In other words, over production time unsteady tablet properties could be obtained which could bear the risk to fail in meeting the quality requirements [1]. With the help of numerical simulations, the QbD approach [2] could be integrated into the tablet production process by e.g. adapting the compression forces of upper and lower punch over production time to compensate the differing material properties.

## 4 SUMMARY AND CONCLUSION

This is the first study visualizing the die filling process by numerical means within an actual lab-scale rotary tablet press. Material properties, in particular particle size distribution, adapted to model a DC formulation of low API content and calibrated micro-mechanical properties were used.

Supported by basic metrics such as particle size distribution and mass hold up within the system (reported in [8]), powder flow phenomena could be elucidated by particles coloring analysis. Within the Fill-O-Matic three different main phenomena were demonstrated.

(1) Within the feeding hopper, a gradient across the radius of the hopper was found, showing a dead zone in the left half. Particles remain there almost stagnant over the complete discharge time bearing the risk of consolidation and solely particles from right half contribute to particles refeeding. (2) The different mass throughput of filling and reverse dosing wheel zone implicate a significantly altered refeeding rate from the dosing wheel zone. (3) The third phenomenon is provided by an intersection between filling and reverse dosing wheel zone enabling a free mass transfer from the reverse dosing into the filling wheel zone. In addition to this intermixing, particles tend to remain a longer residence time within the reverse dosing wheel zone bearing the risk of particle attrition and over lubrication. Eventually the analysis of colored particles filled into the dies shows that the first filled dies contain particles that have traveled a shorter distance within the system thereby could establish different compressive properties. Tablet quality might change over time constituting challenges to meet the tablet quality requirements of the authorities.

At this given parameter set, powder flow phenomena in different locations of the system were shown. However, in the next step additional setups will be performed according to a design of experiments. They will provide a clear picture on the influence of material properties in combination with process parameters on tablet quality. Eventually, a better understanding and an integrated QbD approach in pharmaceutical tableting can be generated by means of numerical simulation.

## 5 ACKNOWLEDGMENT

The authors would like to thank and acknowledge Mr. Thomas Heinrich (Fette Compacting GmbH, Schwarzenbeck, Germany) and his team for generously providing the FETTE 1200i Fill-O-Matic CAD files.

## 6 REFERENCES

- [1] Ph. Eur. European Pharmacopoeia 9<sup>th</sup> edn, 2017.
- [2] ICH, Guidance for Industry Q8 (R2) pharmaceutical development, 2009.
- [3] Gopireddy, S.R. et al. Numerical simulation of powder flow in a pharmaceutical tablet press lab-scale gravity feeder. *Powder Technol.* (2016) **302**:309-327.
- [4] Hildebrandt, C. et al. Towards the understanding of particle size segregation in a pharmaceutical tablet press lab-scale gravity feeder. Manuscript under preparation.
- [5] Ketterhagen, W.R. Simulation of powder flow in a lab-scale tablet press feed frame: Effects of design and operating parameters on measures of tablet quality. *Powder Technol* (2015) **275**:361-374.
- [6] Mateo-Ortiz, D. et al. Relationship between residence time distribution and forces applied by paddles on powder attrition during the die filling process. *Powder Technol.* (2015) **278**: 111-117.
- [7] Jivray, M. et al. An overview of the different excipients useful for direct compression formulations. *Pharm Sci Technol To* (2007) **3**:58-63.

- [8] Hildebrandt, C. et al. Numerical analysis of the die filling process within a pharmaceutical tableting machine, 8. *Symposium "Produktgestaltung in der Partikeltechnologie"*, Karlsruhe, 2017.
- [9] Zhu, H.P. et al., Discrete particle simulation of particulate systems: theoretical developments. *Chem Eng Sci* (2007) **62**:3378-3396.
- [10] Herrmann, H.J. et al. Modeling of granular media on the computer. *Continuum Mech Therm* (1998) **10**:189-231.
- [11] Ketterhagen, W.R. et al. Process modeling in the pharmaceutical industry using the discrete element method. *J Pharm Sci* (2009) **98**:442-470.
- [12] Kloss, C. et al. Models, algorithms and validation of opensource DEM and CFD-DEM. *Progress in Computational Fluid Dynamics, An International Journal* (2012) **12**:140-152.
- [13] Tang, P. et al. Methods for Minimizing Segregation: A review. *Particul Sci Technol* (2004) **22**:321-337.